Chemical Science

Ti₂S@D₃h-C₇₈

EDGE ARTICLE
Antonio Rodríguez-Fortea, Josep M. Poblet, Luis Echegoyen *et al.*
Ti$_2$S@D_{3h}(24109)-C$_{78}$: a sulfide cluster metallofullerene containing only transition metals inside the cage

Ti$_2$S@D_{3h}(24109)-C$_{78}$: a sulfide cluster metallofullerene containing only transition metals inside the cage†

Fang-Fang Li,[a] Ning Chen,‡[a] Marc Mulet-Gas,[b] Vivian Triana,[a] Jesse Murillo,[a] Antonio Rodríguez-Fortea,*[b] Josep M. Poblet*[b] and Luis Echegoyen*[a]

A new titanium-based sulfide clusterfullerene, Ti$_2$S@D_{3h}(24109)-C$_{78}$, has been successfully synthesized by arc-discharging graphite rods packed with pure TiO$_2$ and graphite powder under an atmosphere of SO$_2$ and helium. Multistage HPLC methods were utilized to isolate and purify the Ti$_2$S@C$_{78}$, and mass spectrometric characterization confirmed the composition of a Ti$_2$S cluster within a C$_{78}$ cage. UV-Vis-NIR absorption spectroscopy, electrochemical characterization and extensive DFT calculations led to the assignment of the cage symmetry to D_{3h}(24109)-C$_{78}$ and suggested an almost linear arrangement of the internal Ti$_2$S cluster, with a formal transfer of six electrons from the cluster to the C$_{78}$ cage.

Introduction

Endohedral metallofullerenes (EMFs) are continuously attracting attention from scientists due to (i) the variable structures induced by combining different encaged clusters with different size/symmetry carbon cages;[1–4] (ii) the interesting electronic properties resulting from charge transfer from the encapsulated moiety to the carbon shell;[1] and (iii) the potential applications of both pristine and functionalized EMFs.[1,5–11] A substantial amount of experimental and theoretical effort has been devoted to studies of EMFs.[12–17]

The cluster metallofullerenes are a special class of EMFs. Since the discovery of the first cluster fullerene, Sc$_3$N@C$_{80}$, with a Sc$_3$N cluster inside a C$_{80}$ cage in 1999,[18] the horizons of this field have been expanded considerably and a new era in the field of EMFs began. Up until now, the types of cluster metallofullerenes reported are nitride cluster metallofullerenes (NCFs, M$_3$N@C$_{2n}$),[1,3,4,18,19] carbide cluster metallofullerenes (CCFs, M$_{2–4}$C$_2$@C$_{2n}$),[1,3,20–24] oxide cluster metallofullerenes (OCFs, M$_x$O$_y$@C$_{2n}$ $x = 2$–4, $y = 1$–3),[1,3,25–27] carbonitride cluster metallofullerenes (CNCFs, M$_3$NC@C$_{2n}$),[3,28,29] hydrocarbide cluster metallofullerenes (HCCFs, M$_3$CH@C$_{2n}$)[3,30] and sulfide cluster metallofullerenes (SCFs, M$_2$S@C$_{2n}$).[31–36] SCFs are the recently developed cluster fullerene family and only a few, such as M$_2$S@C$_{82}$ (M = Sc, Y, Lu, Dy)[31] and Sc$_2$S@C$_{2n}$ (n = 35, 36, 41),[32–34] have been isolated and reported. Most recently, a new type of clusterfullerene, a trimetallofullerene (Sm$_3$@I_h-C$_{80}$) encaging only three metal atoms inside the cage without a non-metal atom was isolated and characterized experimentally.[37] These new fullerenes have yet to be fully explored. Much is still to be discovered by using other metals in the CF synthesis.

All of the reported cluster fullerenes contain encapsulated rare earth metals *i.e.* group-III (Sc, Y, and lanthanides), and there are very few reports of cluster fullerenes with a transition metal trapped inside the carbon cage. In 1992, encaging of only transition metals inside a carbon cage was reported, Ti@C$_{28}$, which was only observed by mass spectrometry.[38,39] In 2001, a titanium carbide cluster fullerene, Ti$_2$@C$_{80}$,[40] whose structure was later determined to be Ti$_2$C$_2$@D_{3h}-C$_{78}$,[41–43] and Ti$_2$@C$_{84}$[44] were isolated and identified. In 2009, Yang and coworkers attempted to synthesize Ti-only nitride cluster fullerenes using pure TiO$_2$, however, no Ti-containing NCFs were detected in the extract. Subsequently, they modified the method using a TiO$_2$–Sc$_2$O$_3$ mixture instead of pure TiO$_2$ and achieved the first mixed metallic nitride cluster fullerene encapsulating Ti, TiSc$_2$N@I_h-C$_{80}$.[45] Following the same synthetic procedure using a TiO$_2$–Y$_2$O$_3$ mixture, TiY$_2$N@I_h-C$_{80}$ was synthesized.[46] On the basis of these results, the synthesis of Ti only NCFs seems impractical using just TiO$_2$, it must be accompanied by rare earth metals such as Sc and Y, and only one Ti atom seems to be encaged. An alternative way to encage a Ti-only cluster could involve the use of a sulfide instead of nitride in this work, thus we used SO$_2$ instead of N$_2$ as a gas source. Here we report the first sulfide clusterfullerene with no rare-earth metals inside the cage, Ti$_2$S@C$_{78}$, where the cage has D_{3h}(24109)-C$_{78}$ symmetry and the Ti$_2$S cluster is almost perfectly linear.

[a]*Department of Chemistry, University of Texas at El Paso, El Paso, Texas 79968, USA. E-mail: echegoyen@utep.edu*

[b]*Departament de Química Física i Inorgànica, Universitat Rovira i Virgili, 43007 Tarragona, Spain. E-mail: antonio.rodriguezf@urv.cat; josepmaria.poblet@urv.cat*

† Electronic supplementary information (ESI) available: Experimental sections and computational results. See DOI: 10.1039/c3sc51124c

‡ Current address: College of Chemistry, Chemical Engineering and Materials Science, Soochow University, Suzhou, Jiangsu, 212163, China. Email: chenning@suda.edu.cn

Results and discussion

Synthesis and isolation of $Ti_2S@C_{78}$

$Ti_2S@C_{78}$ was synthesized in a conventional Krätschmer–Huffman reactor using a TiO_2–graphite powder mixture in a weight ratio of 1 : 4 in a mixture of helium (200 torr) and SO_2 (20 torr) atmosphere. The procedures are very similar to those already described for the synthesis of Sc sulfide cluster fullerenes.[32] The as-produced soot was pre-extracted with ether and further extracted with CS_2 for 4 hours and analyzed by HPLC and MALDI-TOF-MS (matrix-assisted laser desorption ionization time-of-flight mass spectrometry). Fig. 1 shows the initial HPLC of the extract. The MALDI-TOF MS analysis shows that the $Ti_2S@C_{78}$ fraction is overlapped with those of C_{88}, C_{90}, C_{92} and $Ti_2@C_{84}$ as shown in Fig. 1. Multistage HPLC methods were utilized to isolate and purify the $Ti_2S@C_{78}$ (see Fig. S1 in ESI†). The purity of $Ti_2S@C_{78}$ was established using HPLC as an inset in Fig. 1.
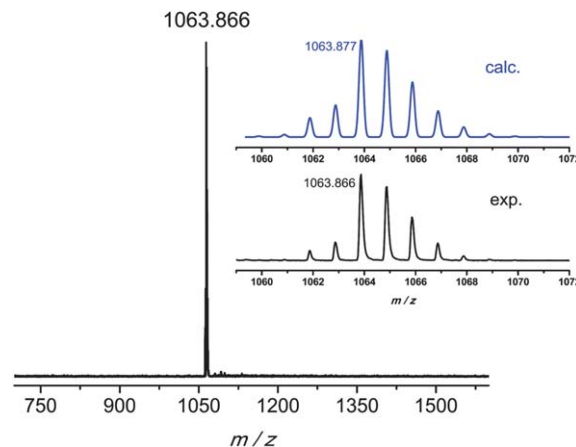
Spectroscopic structure determination of $Ti_2S@C_{78}$

The purified $Ti_2S@C_{78}$ was initially characterized by mass spectrometry. The MALDI-TOF mass spectrum, shown in Fig. 2, shows a single peak with m/z at 1063.866, corresponding to the mass of $Ti_2S@C_{78}$, which also suggests that the sample is reasonably pure. The inset shows the simulated and experimental mass spectra of $Ti_2S@C_{78}$. The experimental isotopic distribution of $Ti_2S@C_{78}$ shows excellent agreement with the theoretical one, further corroborating the composition of $Ti_2S@C_{78}$. Two titanium atoms are successfully stabilized within a fullerene cage in the form of a sulfide cluster. However, we did not observe an extensive family for Ti_2S cluster fullerenes as in the case of sulfide cluster fullerenes ($Sc_2S@C_{2n}$ (n = 35–50)),[32] which indicates once again the difficulties of trapping transition metals inside the carbon cages.

The C_{78} cage can exist in 24109 isomeric forms, with five that obey the isolated pentagon rule (IPR) [D_3(78: 24105), C_{2v}(78: 24106), C_{2v}(78: 24107), D_{3h}(78: 24108), and D_{3h}(78: 24109)].[47] In
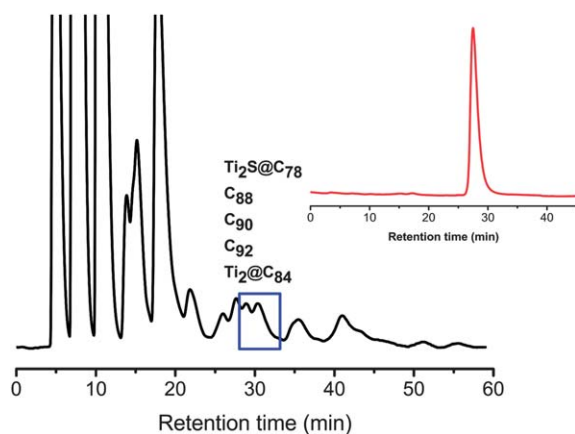
Fig. 2 MALDI-TOF mass spectrum of the HPLC-purified $Ti_2S@C_{78}$. The inset shows the simulated and experimental isotopic distributions for the corresponding $Ti_2S@C_{78}$.

order to help assign the cage isomer, the UV-Vis-NIR spectroscopy was recorded. Shinohara showed that similar UV-Vis-NIR spectra are indicative of EMFs possessing the same cage structures.[48] Popov and Dunsch also reported that similar electronic spectral features indicate the same cage geometry since the electronic absorptions of fullerenes are predominantly due to π–π* carbon cage transitions.[2,4,15] Therefore, UV-Vis-NIR spectroscopy has been extensively used to predict fullerene cage geometries and to probe the electronic structures of endohedral metallofullerenes. Fig. 3 shows the UV-Vis-NIR absorption spectrum of $Ti_2S@C_{78}$. Absorptions at 498, 602, 657, 757 and 896 nm were observed with an onset around 1470 nm, indicating that this titanium sulfide cluster fullerene possesses a small HOMO–LUMO gap. The optical band-gap of $Ti_2S@C_{78}$ is estimated to be 0.84 eV based on the absorption spectral onset which is smaller than that of $Ti_2C_2@C_{78}$.[40] The feature-rich absorptions of $Ti_2S@C_{78}$ resemble those of $Ti_2C_2@D_{3h}$-C_{78}[40] and $Sc_3N@D_{3h}$(24109)-C_{78}[49,50] and are dramatically different from that of $M_3N@C_2$-C_{78} (M = Gd, Sc, Tm, Dy).[29,50,51] In addition, $Ti_2S@C_{78}$ displays the same green color in toluene–CS_2 as $Sc_3N@D_{3h}$(24109)-C_{78} does, which strongly suggests that the geometric and electronic structure of $Ti_2S@C_{78}$ are similar to those of $Sc_3N@D_{3h}$(24109)-C_{78}.[49,50] Based on these observations

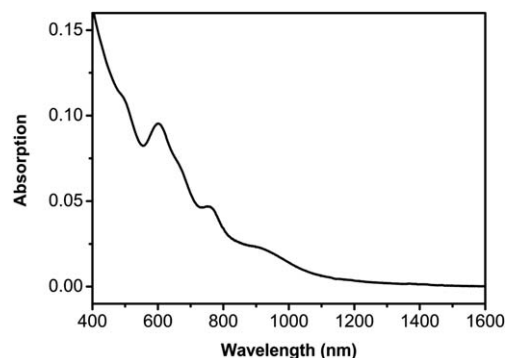**Fig. 1** HPLC chromatogram from the initial extract on a 5PYE column. Inset: HPLC of the purified $Ti_2S@C_{78}$ on a Buckyprep-M column. *Conditions*: λ = 320 nm; mobile phase, toluene; flow rate, 4.00 mL min^{-1}.
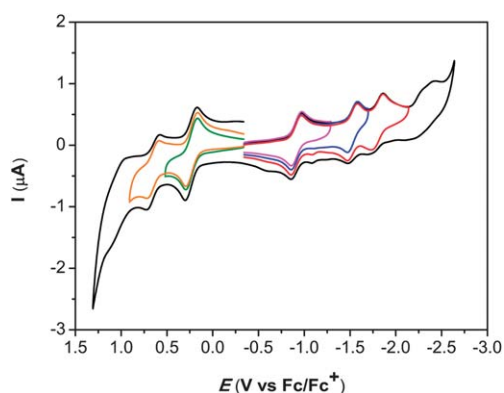

Fig. 3 UV-Vis-NIR spectrum of $Ti_2S@C_{78}$ in toluene.

we assign the D_{3h}(24109) cage symmetry to Ti$_2$S@C$_{78}$, which was also confirmed by theoretical calculations, see below. Multiple attempts to obtain suitable crystal for X-ray diffraction analysis were not successful. Sc$_3$N@D_{3h}(24109)-C$_{78}$ formally undergoes a six-electron transfer from the cluster to the cage.[52] Assuming that a six-electron transfer is present in Ti$_2$S@C$_{78}$, the oxidation state of titanium is Ti^{4+}, not Ti^{3+}, as is the case for Sc$_2$TiN@C$_{80}$[45] and Y$_2$TiN@C$_{80}$.[46] Thus according to the ionic model,[52,53] Ti$_2$S@C$_{78}$ can be formally considered to be (Ti$_2$S)$^{6+}$@D_{3h}(24109)-C$_{78}$$^{6-}$.

Electrochemistry studies

Cyclic voltammetry (CV) is the most common technique used to explore the electrochemical behavior of EMFs. The CV of Ti$_2$S@C$_{78}$ in an o-dichlorobenzene (o-DCB) solution containing 0.05 M tetra-n-butylammonium hexafluorophosphate (n-Bu$_4$NPF$_6$) as the supporting electrolyte is displayed in Fig. 4. Using a scan rate of 100 mV s^{-1}, Ti$_2$S@C$_{78}$ exhibits three reversible reductions with half wave potentials at −0.92, −1.53, and −1.80 V, respectively, *versus* Fc/Fc$^+$ and two additional irreversible reductions with peak potentials at −2.29 and −2.41 V, respectively. In the anodic scan, two reversible oxidation steps with half wave potentials at +0.23 and +0.65 V are observed, along with one quasi-reversible oxidation at +1.03 V *versus* Fc/Fc$^+$.

The electrochemically reversible behavior of Ti$_2$S@D_{3h}-C$_{78}$ is dramatically different from those of most metallic cluster fullerenes which usually display irreversible reductions under the same conditions.[1] TiSc$_2$N@C$_{80}$,[45,54] Sc$_2$S@C$_{72}$[33] and

Sc$_4$O$_2$@C$_{80}$[55] are some of the very few clusterfullerenes with cages ≤C$_{80}$ that exhibit reversible reductions. Although Sc$_3$N@D_{3h}-C$_{78}$ presumably possesses the same cage isomer as Ti$_2$S@D_{3h}-C$_{78}$ does, the CV of Sc$_3$N@D_{3h}-C$_{78}$ shows irreversible reduction steps,[1,56] which indicates that the encaged clusters have a significant influence on the electrochemical behavior. Moreover, the first reduction and the first oxidation potentials of Ti$_2$S@D_{3h}-C$_{78}$ are anodically shifted by 620 mV and 110 mV, respectively, compared with those of Sc$_3$N@D_{3h}-C$_{78}$. Hence, Ti$_2$S@D_{3h}-C$_{78}$ is much easier to reduce and somewhat harder to oxidize than Sc$_3$N@D_{3h}-C$_{78}$. The electrochemical gap of Ti$_2$S@D_{3h}-C$_{78}$, 1.15 V, is 0.51 V less than that of Sc$_3$N@D_{3h}-C$_{78}$ (1.66 V) (Table 1) and is comparable to that of TiSc$_2$N@I_h-C$_{80}$ (1.10 V)[45] (Table 1), which is 0.75/0.76 V less than that of Sc$_3$N@I_h-C$_{80}$ (1.85[57]/1.86 V[58]). Similarly, TiY$_2$N@I_h-C$_{80}$ has an electrochemical gap of 1.11 V[46] (Table 1), which is 0.94 V less than that of the corresponding Y$_3$N@C$_{80}$ (2.05 V).[1,46,59] The electrochemical gap of Ti$_2$S@D_{3h}-C$_{78}$ is also 0.22–0.63 V less than those of the reported Sc$_2$S cluster fullerenes. These results confirm that Ti-containing cluster fullerenes possess smaller electrochemical gaps than the corresponding rare earth metallic cluster fullerenes. Interestingly, the electrochemical and low temperature ESR measurements of TiSc$_2$N@C$_{80}$ conducted by Popov *et al.*[54] have shown that the unpaired electron in TiSc$_2$N@C$_{80}$ is mainly localized on the Ti ion, thus the endohedral TiSc$_2$N cluster is the electrochemically active species. Both reduction and oxidation occurred at the TiSc$_2$N cluster. The results have clearly shown that the redox chemistry of Ti-containing mixed-metal nitride EMFs is controlled by the Ti atom.

Computational studies

An extensive computational analysis§ was conducted to confirm the symmetry of the C$_{78}$ cage that is encapsulating the Ti$_2$S cluster. For the C$_{78}$ family, there are a total of 24109 cage isomers. Among them, we considered all the structures that (i) satisfy the isolated pentagon rule (IPR, 5 isomers); (ii) show one adjacent pentagon pair (APP1, 18 isomers); and (iii) show two pairs of adjacent pentagons (APP2, 228 isomers). The adjacent pentagons, also called pentalene units, are seen to interact with the metal ions of the cluster, thus providing an extra stabilization *via* both ionic and covalent contributions.[60–63] No structures with three or more APPs were considered because they are found at much higher energies and there are only two Ti ions in the cluster able to interact with up to two pentalene units. From the electronic structure of the lowest-energy clusterfullerenes

Fig. 4 Cyclic voltammogram of Ti$_2$S@C$_{78}$ recorded in a 0.05 M o-DCB/n-Bu$_4$NPF$_6$ solution at a scan rate of 100 mV s^{-1}. Ferrocene (Fc) was added as the internal standard.

Table 1 Redox potentials (V *vs.* Fc/Fc$^+$) of Ti$_2$S@D_{3h}-C$_{78}$ along with other related cluster fullerenes

Compounds	$E^{+/2+}$ [V]	$E^{0/+}$ [V]	$E^{0/-}$ [V]	$E^{-/2-}$ [V]	$E^{2-/3-}$ [V]	$E^{3-/4-}$ [V]	$E^{4-/5-}$ [V]	$\Delta E_{gap,ec}$ [V]
Ti$_2$S@D_{3h}-C$_{78}$	+0.65[a]	+0.23[a]	−0.92[a]	−1.53[a]	−1.80[a]	−2.29[b]	−2.41[b]	1.15
Sc$_3$N@D_{3h}-C$_{78}$[56]		+0.12[a]	−1.54[b]					1.66
TiSc$_2$N@I_h-C$_{80}$[45]		+0.16[a]	−0.94[a]	−1.58[a]	−2.21[a]			1.10
TiY$_2$N@I_h-C$_{80}$[46]		+0.00[a]	−1.11[a]	−1.79[b]				1.11

^{a} Half-wave potential (reversible redox process). ^{b} Peak potential (irreversible redox process).
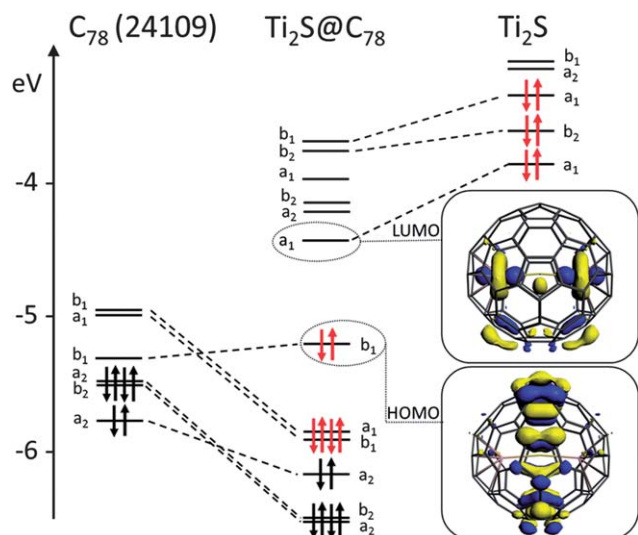
Fig. 5 Orbital interaction diagram for $Ti_2S@D_{3h}$-C_{78}(24109). The fragments, Ti_2S and D_{3h}-C_{78}(24109), were calculated with the same geometry that they have in the clusterfullerene. Six electrons from the neutral Ti_2S cluster (those represented by red arrows) are formally transferred to cage orbitals.

analyzed, we confirmed that there is a formal transfer of six electrons from the Ti_2S cluster to the C_{78} cage, $(Ti_2S)^{6+}@C_{78}^{6-}$, as proposed from the experimental UV-Vis-NIR spectrum (see orbital interaction diagram, Fig. 5). We first computed at the AM1 level the hexaanions for the 251 cages with less than three APPs and then, the lowest-energy hexaanions and the corresponding clusterfullerenes at the DFT level (see Table 2). A correlation between the relative energies of the clusterfullerenes and those of the hexaanions was observed, further confirmation of the validity of the ionic model (see Fig. S2 in ESI†).

Table 2 Relative energies (in kcal mol^{-1}) for several isomers of C_{78} in the hexaanion and endohedral forms^{a,b}

Isomer	Symmetry	APP	C_{78}^{6-}	$Ti_2S@C_{78}$
21828	C_1	2	43.6	68.1
21975	C_1	2	29.8	44.0
21981	C_1	2	31.7	49.9
21982	C_1	2	36.3	54.6
21983	C_1	2	54.4	42.0
22010	C_2	2	15.4	29.2
22033	C_1	2	57.2	72.8
22096	C_1	2	52.2	59.6
22135	C_1	2	36.1	50.5
22590	C_1	2	42.5	51.5
22646	C_1	2	27.3	41.5
23298	C_2	2	39.9	60.1
23349	C_1	1	32.2	38.7
24088	C_{2v}	2	28.4	23.6
24101	C_s	2	65.8	49.5
24105	D_3	0	48.1	78.5
24106	C_{2v}	0	57.0	63.0
24107	C_{2v}	0	23.7	31.6
24108	D_{3h}	0	79.3	104.0
24109	D_{3h}	0	0.0	0.0

^{a} Isomer number according to the spiral algorithm of Fowler and Manolopoulos.[46] ^{b} APP: number of adjacent pentagon pairs.

The clusterfullerene with the D_{3h}-C_{78}(24109) cage was found to be, by a large difference, the one with the lowest energy, see Table 2. This IPR cage shows the maximal separation between pentagons, in good agreement with the rule established by Poblet and co-workers.[61] Other isomers were found to have more than 20 kcal mol^{-1} higher energies (Table 2). Interestingly, the relative energies of clusterfullerenes with respect to $Ti_2S@D_{3h}$-C_{78}(24109) were larger than those computed for the hexaanions. This indicates that there is an extra stabilization of the system due to the favorable interaction between the Ti_2S cluster and the D_{3h}-C_{78}(24109) cage, for which the Ti–S and Ti···C distances are optimal. In fact, the different orientations of the Ti_2S cluster inside the D_{3h}-C_{78}(24109) cage show significant energy differences (up to 30 kcal mol^{-1}, see Table S1 in ESI†), the most favorable being the one with the cluster in an almost collinear position (Ti–S–Ti angle of 172 degrees) with the C_3 axis of the D_{3h}-C_{78}(24109) cage, as shown in Fig. 6. For all cluster fullerenes possessing non-IPR cages, the most favorable orientations of the internal cluster are those in which the Ti atoms are interacting with the pentalene units (see Fig. 6). Therefore, for a given cage, the structure of the Ti_2S cluster adapts in order to (i) optimize the interaction with the fullerene, for example Ti ions pointing to the pentalene units for non-IPR cages; and (ii) minimize the repulsion between formal Ti^{4+} cations, i.e. by assuming a linear Ti–S–Ti arrangement. Cage D_{3h}-C_{78}(24109) satisfies the three required conditions to host the Ti_2S cluster: (i) it is the most suitable isomer to accept the six electron transfer; (ii) it shows optimal Ti···C interactions; and
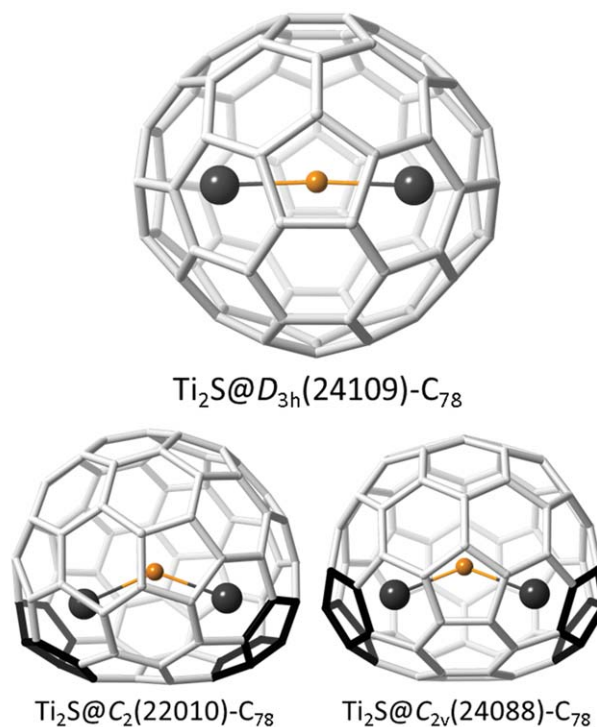
Fig. 6 DFT-optimized structures for the lowest-energy IPR and APP2 $Ti_2S@C_{78}$ cluster fullerenes.

(iii) it allows the internal cluster to be in an almost linear arrangement with maximally separated Ti^{4+} ions.

The orbital interaction diagram for the lowest-energy cluster fullerene $Ti_2S@D_{3h}$-C_{78}(24109), see Fig. 5, verifies that there is a formal transfer of six electrons from the cluster to the cage, $(Ti_2S)^{6+}@C_{78}^{6-}$, as also seen for nitride $Sc_3N@D_{3h}$-C_{78}(24109) and carbide $Ti_2C_2@D_{3h}$-C_{78}(24109). The HOMO is mainly localized on the fullerene. The LUMO, however, has predominant contributions from the Ti_2S cluster; in particular, from the bonding combination of the d_{z^2}-like atomic orbitals of the two Ti ions (Fig. 5). The computed HOMO–LUMO gap for $Ti_2S@D_{3h}$-C_{78}(24109), 0.66 eV, is significantly smaller than the gap for the hexaanionic cage, 1.22 eV. This small HOMO–LUMO gap is in good agreement with the experimental results that show small optical and electrochemical gaps. It is worth remarking here that, given the topology of the frontier orbitals, the oxidation of the clusterfullerene is predicted to take place on the carbon cage. The reduction is, however, predicted to happen in *cavea*, *i.e.* in the internal cluster, as in $M_2@C_{80}$ (M = La, Ce)[64,65] or $TiM_2N@C_{80}$ (M = Sc, Y).[45,46] Since the formal oxidation state of Ti is +4 in $Ti_2S@C_{78}$, the oxidation process of the endohedral cannot be based on the Ti centers, so the Ti atoms control only the reduction processes in this case, in contrast with the redox results reported by Popov and Dunsch for $TiSc_2N@C_{80}$, where the Ti^{3+} centers are responsible for both the reductive and oxidative electrochemical behavior.[54] Computed oxidation and reduction potentials agree reasonably well with the experimental values measured by cyclic voltammetry. The first anodic potential is predicted at +0.08 V, in rather good agreement with the measured half-wave potential, +0.23 V (Table 3). The predicted first cathodic potential, −1.02 V, is also close to the experimental value with a difference of only 100 mV (Table 3). Computation of the spin density for the singly reduced $Ti_2S@D_{3h}$-C_{78}^- confirms that reduction takes place in the internal cluster (see Fig. S3 in ESI†). The computed electrochemical (EC) gap, 1.10 V, also compares very well with the experimental value, 1.15 V. We have been able to compute the second oxidation potential, at 0.56 V, which is within less than 100 mV from the experimental value (Table 3).

The molar fractions of the lowest-energy $Ti_2S@C_{78}$ isomers as a function of the temperature were also computed using the rigid rotor and harmonic oscillator (RRHO) approximation and the related free-encapsulating model (FEM) as proposed by Slanina.[66,67] The two approximations provide the same predictions, *i.e.* $Ti_2S@D_{3h}$-C_{78}(24109) is the most abundant isomer for the whole temperature range up to 4000 K (see Fig. S4 in ESI†). Acceptable agreement is also observed with the experimental UV-Vis-NIR spectrum. We have computed it for $Ti_2S@D_{3h}$-C_{78}(24109) using time-dependent (TD) DFT in the Vis-NIR region, for wavelengths larger than 450 nm. Despite the systematic underestimation of excitation energies by TD-DFT, this methodology provides reasonable agreement with experimental results for the family of SCFs.[33,34] The lowest-energy transitions, which are fingerprints of $Ti_2S@D_{3h}$-C_{78}(24109) due to the titanium-based character of the LUMO orbitals, are predicted at rather large wavelengths, in good agreement with the large spectral onset obtained from the experiments (1470 nm, see Table S2 in ESI†). The feature-rich absorption region of $Ti_2S@C_{78}$ at lower wavelengths, which resembles that of $Ti_2C_2@D_{3h}$-C_{78} and $Sc_3N@D_{3h}$-C_{78} and is due to cage-to-cage transitions, is rather well reproduced at the TD-DFT level, both the position of the peaks as well as their relative intensities (see Fig. S5 in ESI†).

Conclusion

In summary, a sulfide cluster metallofullerene containing only transition metals inside the cage, $Ti_2S@D_{3h}$-C_{78}(24109), has been successfully synthesized using SO_2 as a source in a Krätschmer–Huffman DC-arc reactor. The new clusterfullerene was characterized by mass spectrometry, UV-Vis-NIR absorption spectroscopy, cyclic voltammetry and DFT calculations. Based on the experimental and computational studies, the cage symmetry was unambiguously assigned to D_{3h}-C_{78}(24109), the most stable cage for both empty C_{78}^{6-} and $Ti_2S@C_{78}$. The endohedral Ti_2S cluster has a nearly linear geometry and transfers six electrons to the C_{78} cage. Surprisingly, $Ti_2S@D_{3h}$-C_{78}(24109) exhibits both electrochemically reversible cathodic and anodic behavior, and a small electrochemical gap, which are remarkably different from those of the corresponding rare earth metallic cluster fullerenes.

Acknowledgements

Notes and references

§ The calculations were conducted using DFT methodology with the ADF 2010 package.[68] The exchange–correlation functionals of Becke and Perdew were used.[69,70] Relativistic corrections were included by means of the ZORA formalism. Slater triple-zeta polarization basis sets were employed to describe the valence electrons of C, S and Ti. Frozen cores consisting of the 1s shell for C and the 1s and 2p shells for S and Ti were described by means of single Slater functions. The computational study of the UV-Vis-NIR spectra has been performed using TDDFT methodology (also at BP86/TZP level).

Table 3 Experimental and computed oxidation and reduction potentials (in V *versus* Fc⁺/Fc), as well as the computed HOMO–LUMO gap (in eV) for $Ti_2S@D_{3h}$-C_{78}

	$E^{+/2+}$	$E^{0/+}$	$E^{0/-}$	$\Delta E_{gap,ec}$	H–L$_{gap}$
Experimental	+0.65	+0.23	−0.92	1.15	
Computed	+0.56	+0.08	−1.02	1.10	0.66

1 M. N. Chaur, F. Melin, A. L. Ortiz and L. Echegoyen, *Angew. Chem., Int. Ed.*, 2009, **48**, 7514–7538.

2 L. Dunsch and S. Yang, *Phys. Chem. Chem. Phys.*, 2007, **9**, 3067–3081.

3 S. Yang, F. Liu, C. Chen, M. Jiao and T. Wei, *Chem. Commun.*, 2011, **47**, 11822–11839.

4 L. Dunsch and S. Yang, *Small*, 2007, **3**, 1298–1320.

5 R. B. Ross, C. M. Cardona, D. M. Guldi, S. G. Sankaranarayanan, M. O. Reese, N. Kopidakis, J. Peet, B. Walker, G. C. Bazan, E. Van Keuren, B. C. Holloway and M. Drees, *Nat. Mater.*, 2009, **8**, 208–212.

6 J. R. Pinzón, M. E. Plonska-Brzezinska, C. M. Cardona, A. J. Athans, S. S. Gayathri, D. M. Guldi, M. Á. Herranz, N. Martín, T. Torres and L. Echegoyen, *Angew. Chem., Int. Ed.*, 2008, **47**, 4173–4176.

7 M. D. Shultz, J. C. Duchamp, J. D. Wilson, C.-Y. Shu, J. Ge, J. Zhang, H. W. Gibson, H. L. Fillmore, J. I. Hirsch, H. C. Dorn and P. P. Fatouros, *J. Am. Chem. Soc.*, 2010, **132**, 4980–4981.

8 E. B. Iezzi, J. C. Duchamp, K. R. Fletcher, T. E. Glass and H. C. Dorn, *Nano Lett.*, 2002, **2**, 1187–1190.

9 R. B. Ross, C. M. Cardona, F. B. Swain, D. M. Guldi, S. G. Sankaranarayanan, E. Van Keuren, B. C. Holloway and M. Drees, *Adv. Funct. Mater.*, 2009, **19**, 2332–2337.

10 C. Shu, W. Xu, C. Slebodnick, H. Champion, W. Fu, J. E. Reid, H. Azurmendi, C. Wang, K. Harich, H. C. Dorn and H. W. Gibson, *Org. Lett.*, 2009, **11**, 1753–1756.

11 C. Y. Shu, X. Y. Ma, J. F. Zhang, F. D. Corwin, J. H. Sim, E. Y. Zhang, H. C. Dorn, H. W. Gibson, P. P. Fatouros, C. R. Wang and X. H. Fang, *Bioconjugate Chem.*, 2008, **19**, 651–655.

12 A. A. Popov and L. Dunsch, *Chem.–Eur. J.*, 2009, **15**, 9707–9729.

13 A. Rodriguez-Fortea, A. L. Balch and J. M. Poblet, *Chem. Soc. Rev.*, 2011, **40**, 3551–3563.

14 M. Yamada, T. Akasaka and S. Nagase, *Acc. Chem. Res.*, 2009, **43**, 92–102.

15 A. A. Popov, S. M. Avdoshenko, A. M. Pendas and L. Dunsch, *Chem. Commun.*, 2012, **48**, 8031–8050.

16 S. Osuna, M. Swart and M. Sola, *Phys. Chem. Chem. Phys.*, 2011, **13**, 3585–3603.

17 X. Lu, T. Akasaka and S. Nagase, *Chem. Commun.*, 2011, **47**, 5942–5957.

18 S. Stevenson, G. Rice, T. Glass, K. Harich, F. Cromer, M. R. Jordan, J. Craft, E. Hadju, R. Bible, M. M. Olmstead, K. Maitra, A. J. Fisher, A. L. Balch and H. C. Dorn, *Nature*, 1999, **401**, 55–57.

19 S. Stevenson, P. W. Fowler, T. Heine, J. C. Duchamp, G. Rice, T. Glass, K. Harich, E. Hajdu, R. Bible and H. C. Dorn, *Nature*, 2000, **408**, 427–428.

20 C.-R. Wang, T. Kai, T. Tomiyama, T. Yoshida, Y. Kobayashi, E. Nishibori, M. Takata, M. Sakata and H. Shinohara, *Angew. Chem., Int. Ed.*, 2001, **40**, 397–399.

21 Z.-Q. Shi, X. Wu, C.-R. Wang, X. Lu and H. Shinohara, *Angew. Chem., Int. Ed.*, 2006, **45**, 2107–2111.

22 Y. Iiduka, T. Wakahara, T. Nakahodo, T. Tsuchiya, A. Sakuraba, Y. Maeda, T. Akasaka, K. Yoza, E. Horn, T. Kato, M. T. H. Liu, N. Mizorogi, K. Kobayashi and S. Nagase, *J. Am. Chem. Soc.*, 2005, **127**, 12500–12501.

23 H. Yang, C. Lu, Z. Liu, H. Jin, Y. Che, M. M. Olmstead and A. L. Balch, *J. Am. Chem. Soc.*, 2008, **130**, 17296–17300.

24 T.-S. Wang, N. Chen, J.-F. Xiang, B. Li, J.-Y. Wu, W. Xu, L. Jiang, K. Tan, C.-Y. Shu, X. Lu and C.-R. Wang, *J. Am. Chem. Soc.*, 2009, **131**, 16646–16647.

25 S. Stevenson, M. A. Mackey, M. A. Stuart, J. P. Phillips, M. L. Easterling, C. J. Chancellor, M. M. Olmstead and A. L. Balch, *J. Am. Chem. Soc.*, 2008, **130**, 11844–11845.

26 R. Valencia, A. Rodríguez-Fortea, S. Stevenson, A. L. Balch and J. M. Poblet, *Inorg. Chem.*, 2009, **48**, 5957–5961.

27 B. Q. Mercado, M. M. Olmstead, C. M. Beavers, M. L. Easterling, S. Stevenson, M. A. Mackey, C. E. Coumbe, J. D. Phillips, J. P. Phillips, J. M. Poblet and A. L. Balch, *Chem. Commun.*, 2010, **46**, 279–281.

28 T.-S. Wang, L. Feng, J.-Y. Wu, W. Xu, J.-F. Xiang, K. Tan, Y.-H. Ma, J.-P. Zheng, L. Jiang, X. Lu, C.-Y. Shu and C.-R. Wang, *J. Am. Chem. Soc.*, 2010, **132**, 16362–16364.

29 J. Wu, T. Wang, Y. Ma, L. Jiang, C. Shu and C. Wang, *J. Phys. Chem. C*, 2011, **115**, 23755–23759.

30 M. Krause, F. Ziegs, A. A. Popov and L. Dunsch, *ChemPhysChem*, 2007, **8**, 537–540.

31 L. Dunsch, S. Yang, L. Zhang, A. Svitova, S. Oswald and A. A. Popov, *J. Am. Chem. Soc.*, 2010, **132**, 5413–5421.

32 N. Chen, M. N. Chaur, C. Moore, J. R. Pinzon, R. Valencia, A. Rodriguez-Fortea, J. M. Poblet and L. Echegoyen, *Chem. Commun.*, 2010, **46**, 4818–4820.

33 N. Chen, C. M. Beavers, M. Mulet-Gas, A. Rodríguez-Fortea, E. J. Munoz, Y.-Y. Li, M. M. Olmstead, A. L. Balch, J. M. Poblet and L. Echegoyen, *J. Am. Chem. Soc.*, 2012, **134**, 7851–7860.

34 N. Chen, M. Mulet-Gas, Y.-Y. Li, R. E. Stene, C. W. Atherton, A. Rodriguez-Fortea, J. M. Poblet and L. Echegoyen, *Chem. Sci.*, 2013, **4**, 180–186.

35 B. Q. Mercado, N. Chen, A. Rodríguez-Fortea, M. A. Mackey, S. Stevenson, L. Echegoyen, J. M. Poblet, M. M. Olmstead and A. L. Balch, *J. Am. Chem. Soc.*, 2011, **133**, 6752–6760.

36 L.-H. Gan, Q. Chang, C. Zhao and C.-R. Wang, *Chem. Phys. Lett.*, 2013, **570**, 121–124.

37 W. Xu, L. Feng, M. Calvaresi, J. Liu, Y. Liu, B. Niu, Z. Shi, Y. Lian and F. Zerbetto, *J. Am. Chem. Soc.*, 2013, **135**, 4187–4190.

38 T. Guo, M. D. Diener, Y. Chai, M. J. Alford, R. E. Haufler, S. M. McClure, T. Ohno, J. H. Weaver, G. E. Scuseria and R. E. Smalley, *Science*, 1992, **257**, 1661–1664.

39 B. I. Dunlap, O. D. Haeberlen and N. Roesch, *J. Phys. Chem.*, 1992, **96**, 9095–9097.

40 B. Cao, M. Hasegawa, K. Okada, T. Tomiyama, T. Okazaki, K. Suenaga and H. Shinohara, *J. Am. Chem. Soc.*, 2001, **123**, 9679–9680.

41 T. Yumura, Y. Sato, K. Suenaga and S. Iijima, *J. Phys. Chem. B*, 2005, **109**, 20251–20255.

42 K. Tan and X. Lu, *Chem. Commun.*, 2005, 4444–4446.

43 Y. Sato, T. Yumura, K. Suenaga, H. Moribe, D. Nishide, M. Ishida, H. Shinohara and S. Iijima, *Phys. Rev. B: Condens. Matter Mater. Phys.*, 2006, **73**, 193401.

44 B. Cao, K. Suenaga, T. Okazaki and H. Shinohara, *J. Phys. Chem. B*, 2002, **106**, 9295–9298.

45 S. Yang, C. Chen, A. A. Popov, W. Zhang, F. Liu and L. Dunsch, *Chem. Commun.*, 2009, 6391–6393.

46 C. Chen, F. Liu, S. Li, N. Wang, A. A. Popov, M. Jiao, T. Wei, Q. Li, L. Dunsch and S. Yang, *Inorg. Chem.*, 2012, **51**, 3039–3045.

47 P. W. Fowler and D. E. Manolopoulos, *An Atlas of Fullerenes*, Oxford University Press, Oxford, 1995.

48 H. Shinohara, *Rep. Prog. Phys.*, 2000, **63**, 843.

49 M. M. Olmstead, A. de Bettencourt-Dias, J. C. Duchamp, S. Stevenson, D. Marciu, H. C. Dorn and A. L. Balch, *Angew. Chem., Int. Ed.*, 2001, **40**, 1223–1225.

50 A. A. Popov, M. Krause, S. Yang, J. Wong and L. Dunsch, *J. Phys. Chem. B*, 2007, **111**, 3363–3369.

51 C. M. Beavers, M. N. Chaur, M. M. Olmstead, L. Echegoyen and A. L. Balch, *J. Am. Chem. Soc.*, 2009, **131**, 11519–11524.

52 J. M. Campanera, C. Bo and J. M. Poblet, *Angew. Chem., Int. Ed.*, 2005, **44**, 7230–7233.

53 M. N. Chaur, R. Valencia, A. Rodriguez-Fortea, J. M. Poblet and L. Echegoyen, *Angew. Chem., Int. Ed.*, 2009, **48**, 1425–1428.

54 A. A. Popov, C. B. Chen, S. F. Yang, F. Lipps and L. Dunsch, *ACS Nano*, 2010, **4**, 4857–4871.

55 A. A. Popov, N. Chen, J. R. Pinzón, S. Stevenson, L. A. Echegoyen and L. Dunsch, *J. Am. Chem. Soc.*, 2012, **134**, 19607–19618.

56 T. Cai, L. Xu, C. Shu, H. A. Champion, J. E. Reid, C. Anklin, M. R. Anderson, H. W. Gibson and H. C. Dorn, *J. Am. Chem. Soc.*, 2008, **130**, 2136–2137.

57 B. Elliott, L. Yu and L. Echegoyen, *J. Am. Chem. Soc.*, 2005, **127**, 10885–10888.

58 M. Krause and L. Dunsch, *ChemPhysChem*, 2004, **5**, 1445–1449.

59 C. M. Cardona, B. Elliott and L. Echegoyen, *J. Am. Chem. Soc.*, 2006, **128**, 6480–6485.

60 Y.-Z. Tan, S.-Y. Xie, R.-B. Huang and L.-S. Zheng, *Nat. Chem.*, 2009, **1**, 450–460.

61 A. Rodríguez-Fortea, N. Alegret, A. L. Balch and J. M. Poblet, *Nat. Chem.*, 2010, **2**, 955–961.

62 A. A. Popov, *J. Comput. Theor. Nanosci.*, 2009, **6**, 292–317.

63 J. M. Campanera, C. Bo, M. M. Olmstead, A. L. Balch and J. M. Poblet, *J. Phys. Chem. A*, 2002, **106**, 12356–12364.

64 T. Suzuki, Y. Maruyama, T. Kato, K. Kikuchi, Y. Nakao, Y. Achiba, K. Kobayashi and S. Nagase, *Angew. Chem., Int. Ed. Engl.*, 1995, **34**, 1094–1096.

65 M. Yamada, N. Mizorogi, T. Tsuchiya, T. Akasaka and S. Nagase, *Chem.–Eur. J.*, 2009, **15**, 9486–9493.

66 Z. Slanina, S.-L. Lee, F. Uhlík, L. Adamowicz and S. Nagase, *Theor. Chem. Acc.*, 2007, **117**, 315–322.

67 Z. Slanina and S. Nagase, *ChemPhysChem*, 2005, **6**, 2060–2063.

68 G. te Velde, F. M. Bickelhaupt, E. J. Baerends, C. Fonseca Guerra, S. J. A. van Gisbergen, J. G. Snijders and T. Ziegler, *J. Comput. Chem.*, 2001, **22**, 931–967.

69 A. D. Becke, *Phys. Rev. A*, 1988, **38**, 3098–3100.

70 J. P. Perdew, *Phys. Rev. B: Condens. Matter Mater. Phys.*, 1986, **33**, 8822–8824.